Structure of fenchone by broadband rotational spectroscopy

Donatella Loru, Miguel A. Bermúdez, and M. Eugenia Sanz

Articles you may be interested in

Spectroscopic study on deuterated benzenes. I. Microwave spectra and molecular structure in the ground state
J. Chem. Phys. **143**, 244302 (2015); 10.1063/1.4937949

Distortion of ethyne on coordination to silver acetylide, C2H2···AgCCH, characterised by broadband rotational spectroscopy and ab initio calculations
J. Chem. Phys. **140**, 124310 (2014); 10.1063/1.4868035

Rotational spectroscopy and molecular structure of 1,1,2-trifluoroethylene and the 1,1,2-trifluoroethylene-hydrogen fluoride complex
J. Chem. Phys. **126**, 114310 (2007); 10.1063/1.2710276

Determination of structural parameters for ferrocenecarboxaldehyde using Fourier transform microwave spectroscopy
J. Chem. Phys. **123**, 054317 (2005); 10.1063/1.1993593

Microwave spectra, density functional theory calculations and molecular structure of acetylenemethyldioxorhenium
J. Chem. Phys. **113**, 7891 (2000); 10.1063/1.1315611

Structure of fenchone by broadband rotational spectroscopy

Donatella Loru, Miguel A. Bermúdez, and M. Eugenia Sanz
Department of Chemistry, King's College London, London SE1 1DB, United Kingdom

The bicyclic terpenoid fenchone ($C_{10}H_{16}O$, 1,3,3-trimethylbicyclo[2.2.1]heptan-2-one) has been investigated by chirped pulse Fourier transform microwave spectroscopy in the 2-8 GHz frequency region. The parent species and all heavy atom isotopologues have been observed in their natural abundance. The experimental rotational constants of all isotopic species observed have been determined and used to obtain the substitution (r_s) and effective (r_0) structures of fenchone. Calculations at the B3LYP, M06-2X, and MP2 levels of theory with different basis sets were carried out to check their performance against experimental results. The structure of fenchone has been compared with those of norbornane (bicyclo[2.2.1]heptane) and the norbornane derivatives camphor (1,7,7-trimethylbicyclo[2.2.1]heptan-2-one) and camphene (3,3-dimethyl-2-methylenebicyclo[2.2.1]heptane), both with substituents at C_2. The structure of fenchone is remarkably similar to those of camphor and camphene. Comparison with camphor allows identification of changes in ∠CCC angles due to the different position of the methyl groups. All norbornane derivatives display similar structural changes with respect to norbornane. These changes mainly affect the bond lengths and angles of the six-membered rings, indicating that the substituent at C_2 drives structural adjustments to minimise ring strain after its introduction. *Published by AIP Publishing.* [http://dx.doi.org/10.1063/1.4961018]

I. INTRODUCTION

Terpenoids, formed by the aggregation of two or more isoprene (2-methylbutadiene) units, are a large class of natural products with relevance in fields such as drug development,[1,2] the flavour and fragance industries,[3] and the environment.[4] Terpenoids have a wide range of biological activities, including antimicrobial, antitumor, and anti-inflammatory, and are used against diseases caused by viruses and bacteria.[1,5] Artemisin, used against malaria, and paclitaxel (Taxol®), used for cancer treatment, are probably the best known examples of terpenoid drugs. Due to their properties, development of new routes to synthesise terpenoids with known therapeutic activities and production of new terpenoid derivatives are bustling areas of research. Many terpenoids are produced by plants and emitted to the atmosphere, where they undergo several transformations reacting with available radicals and give rise to secondary organic aerosols (SOAs).[6] SOAs constitute a large fraction of organic particulate matter suspended in air and are known to contribute to air pollution and to affect the climate by producing a net cooling of the atmosphere.[4,6] In addition, terpenoids are volatile compounds with characteristic smells and are used as perfume ingredients.[3] A detailed analysis of the structure of terpenoids is essential to describe accurately their role in the biological and environmental processes in which they participate.

Here we present the structural investigation of the bicyclic monoterpenoid fenchone ($C_{10}H_{16}O$, 1,3,3-trimethylbicyclo[2.2.1]heptan-2-one, see Fig. 1) using broadband rotational spectroscopy.[7] Fenchone is one of the main components of the essential oils of fennel, cedar leaf, and lavender. It has a camphoraceous sweet smell in addition to antibacterial and anticorrosive properties,[8,9] and so it is used as odorant in household products and as pesticide. Both natural and anthropogenic sources emit fenchone to the troposphere, where it is removed mainly through reactions with OH radicals.[10] Structurally, fenchone is a substituted norbornane with a ketone functional group and three additional methyl groups. Although several monoterpenoids have been investigated by rotational spectroscopy, such as carvone,[11] limonene,[11] thymol,[12] menthone,[13] linalool,[14] and others,[15] there is much less information on monoterpenoids derived from norbornane with a [2.2.1] bicyclic structure. Only the structures of camphor[16] ($C_{10}H_{16}O$, 1,7,7-trimethylbicyclo[2.2.1]heptan-2-one), an isomer of fenchone, and camphene[17] ($C_{10}H_{16}$, 3,3-dimethyl-2-methylenebicyclo[2.2.1]heptane) have been reported. Norbornanes are known for their strained bonds and angles, as they are constrained to have the cyclohexane ring in an envelope configuration, which gives rise to high reactivity.[18] Determining the structure of fenchone is relevant to model properly its interactions with other molecules and its kinetics, and it can shed light on the strains and reaction outcomes of substituted norbornanes.

Rotational spectroscopy is a powerful structural technique, able to discriminate minute changes in mass distribution and yield positive identifications of conformers and tautomers of a wide range of molecular systems.[19–21] In this work broadband rotational spectroscopy[7] has been used to characterise the structure of fenchone. With this
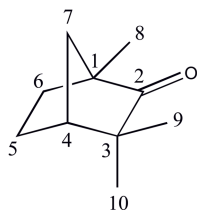
FIG. 1. Scheme of the molecular structure of fenchone and numbering of the carbon atoms.

technique, large portions of the rotational spectrum of a molecule can be collected at once, which facilitates the identification of spectral patterns and reduces acquisition time. It also aids the observation of isotopologues in their natural abundance if the rotational spectrum is sufficiently intense. Analysis of the data obtained from the rotational spectrum leads to the determination of experimental bond lengths and angles, which can then be compared with theoretically predicted ones to benchmark theoretical methods.[22]

The bicyclic structure of fenchone does not allow for torsional flexibility and therefore fenchone is expected to present one conformation. Examination of the rotational spectrum of fenchone led to the identification of transitions corresponding to the parent and all heavy atom isotopologues and confirmed the presence of only one structure. No splittings due to the internal rotation of the methyl groups of fenchone have been observed in its rotational spectrum. The height of the internal rotation barriers has been investigated theoretically and found to be in agreement with observations. The rotational constants of all observed species have been used to determine the substitution (r_s) and effective (r_0) structures of fenchone. These structures have been compared with those calculated by theoretical methods and with the crystal structure of fenchone obtained by X-ray diffraction.[23] Our results are also compared with those obtained for related terpenoids.

II. EXPERIMENTAL

The rotational spectrum of fenchone was recorded using our chirped-pulse Fourier transform microwave spectrometer at King's College London, which operates in the 2-8 GHz frequency range. The design of the instrument (see scheme in Fig. 2) basically follows that previously described by Neill *et al.*[24]

In our spectrometer microwave excitation chirped pulses, varying linearly in frequency from 2 to 8 GHz and spanning 1-5 μs, are created by a 24 GS/s arbitrary waveform generator (Tektronix AWG 7122C). The chirped pulse power is controlled by variable attenuators (Agilent 8494B), input into a 200 W pulsed travelling wave tube amplifier (TWTA, IFI GT82-200), and broadcast into the vacuum chamber using standard horn antennas (A-INFO LB-2060-H) separated approximately 40 cm.

In the vacuum chamber the microwave pulse interacts with the a supersonic jet of our sample molecules seeded
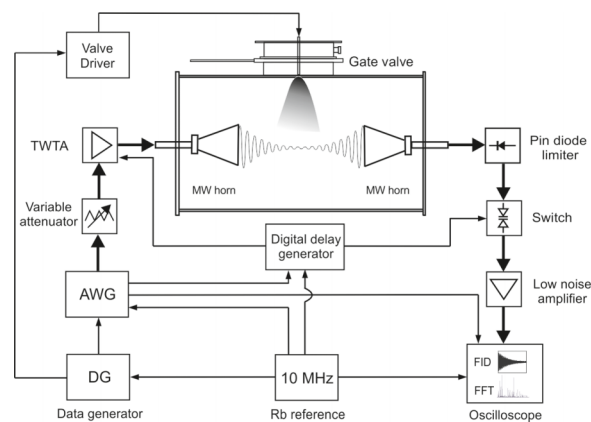

FIG. 2. Scheme of the 2-8 GHz broadband rotational spectrometer at King's College London. Thick lines indicate microwave radiation.

in a carrier gas, which is formed after expansion through a solenoid valve of 1 mm diameter (General Valve series 9). The valve is actuated by a valve driver (IOTA ONE, Parker Hannifin), triggered by a data generator (Tektronix DG2040) which also triggers the arbitrary waveform generator. Once the microwave radiation stops, the molecular emission signal is collected by the second horn antenna, amplified by a low noise amplifier (CIAO wireless, CA28-4441B), and digitised in the time domain by a 100 GS/s oscilloscope (Tektronix DPO71604C). The detection branch of the electronics is protected from accidental damage by a pin diode (Advanced Control Components ACLM-4540) and a microwave switch (Advanced Control Components S1S3R) positioned in front of the low noise amplifier. All frequency and trigger sources as well as the digital oscilloscope are phase locked to a 10 MHz rubidium frequency standard (SRS FS725).

Fenchone (Sigma-Aldrich, 98%) was used without any further purification. It is a liquid at room temperature with low vapour pressure (1 mm Hg at 301 K), and so gentle heating was used to increase the concentration of the sample in the gas phase. Fenchone was placed in a bespoke heating reservoir attached to the nozzle. The optimal temperature for vaporisation was determined by performing tests at different temperatures monitoring the intensity of the spectrum (see Fig. 3), and it was found to be ca. 343 K.

Vaporised fenchone was seeded in neon at backing pressures of ca. 5 bars. Typically molecular pulses of 1100 μs were used to produce the supersonic jet of fenchone in our vacuum chamber. Microwave chirped pulses of 4 μs were applied with a delay of 1400 μs with respect to the start of the molecular pulse. Molecular relaxation signals were collected for 15 μs using the digital oscilloscope and converted into the frequency domain through a fast Fourier-transform algorithm using a Kaiser-Bessel window. The microwave radiation is perpendicular to the supersonic jet in our setup, and therefore the transit time of the molecules through the interacting region with the radiation is short, which results in lines with FWHM ~110 kHz with the settings above.
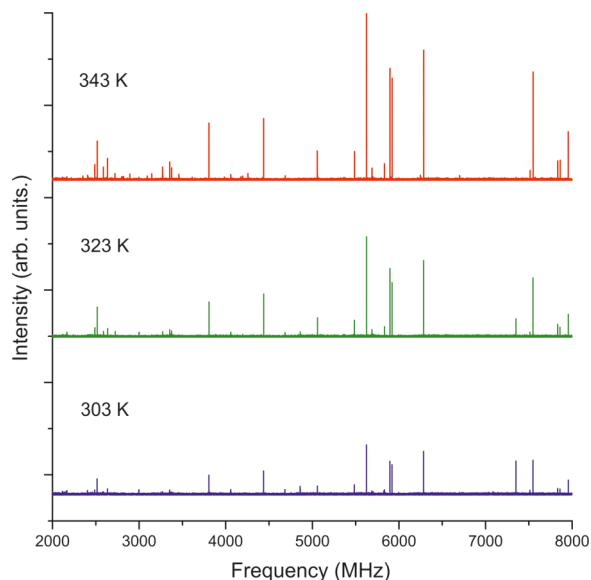
FIG. 3. Broadband rotational spectra of fenchone (500 FIDs) collected at 303 K, 323 K, and 343 K. All traces have the same scale in the y axis.

III. RESULTS

A. Rotational spectrum

The broadband rotational spectrum of fenchone in the 2-8 GHz frequency region (see Figs. 3 and 4) shows several very prominent lines and hundreds of less intense lines that are revealed when the spectrum is magnified. Fenchone is a highly asymmetric top, with the main component of the dipole moment expected to lie along the b inertial axes, and therefore we first looked for R-branch b-type transitions of the series $J'_{1,J'} \leftarrow J''_{0,J''}$ and $J'_{0,J'} \leftarrow J''_{1,J''}$. The $J'_{1,J'} \leftarrow J''_{0,J''}$ and $J'_{0,J'} \leftarrow J''_{1,J''}$ transitions are separated by approximately $2C$ and $2B$, respectively, although considering the asymmetry of fenchone we expected these separations to hold only loosely and for low J transitions.[25] Once these lines were identified (see Fig. 4) and fitted to yield an initial set of rotational constants, further prediction and measurement of transitions confirmed the original assignment. The final set of measured
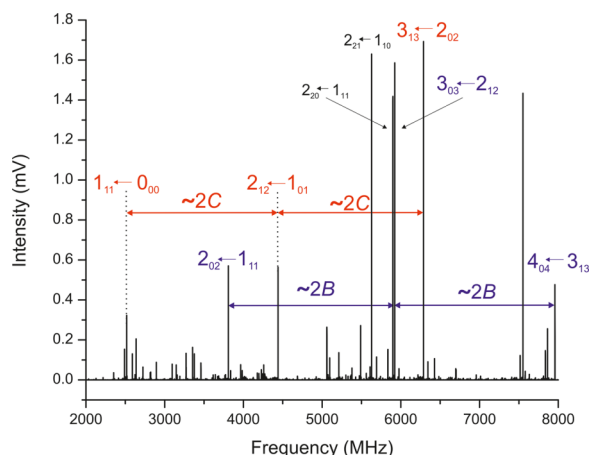
a-, b-, and c-type transitions (Table S1 of the supplementary material) were fit using the Watson Hamiltonian in the A reduction and I^r representation[26] and Pickett's program[27] to give the rotational and quartic centrifugal distortion constants in Table I. The centrifugal distortion constants are quite small, which is an indication of the rigidity of fenchone. Similar values of the centrifugal distortion constants have been obtained for the related terpenoids camphor[16] and camphene.[17]

The experimental rotational constants can be compared with those predicted from theory to benchmark performance. Geometry optimizations of fenchone were carried out using density functional theory, with the B3LYP and M06-2X functionals, and *ab initio* calculations using the Moller-Plesset perturbation theory to second order (MP2). Pople's 6-311G++(d,p) basis set and the Dunning basis sets cc-pVTZ and aug-cc-pVTZ were used with all methods. From the data in Table II, the best agreement with the experimental rotational constants is provided by calculations at the MP2/6-311++G(d,p) level.

Many transitions of fenchone have S/N ratios of 1000/1 and above and show a number of lines at lower frequencies with about one hundredth of the intensity (see Fig. 5). These lines were identified as belonging to the ten possible ^{13}C isotopologues and the ^{18}O isotopologue in their natural abundance (1.1% and 0.2%, respectively). For all of them b- and c-type transitions were measured (see Tables S2-S12 in the supplementary material) and fitted using the same procedure as for the parent species to yield the rotational constants in Table III. In all fits the centrifugal distortion constants were fixed to those determined for parent fenchone.

Fenchone presents three non-equivalent methyl groups, which can potentially produce splittings in the rotational transitions through the coupling of their internal rotation to the overall rotation. No splittings due to internal rotation were observed in the spectrum of fenchone, suggesting that the barriers hindering internal rotation were relatively high. This was further confirmed by performing scans of the relevant

FIG. 4. Broadband rotational spectrum of fenchone (300k FIDs) in the 2-8 GHz frequency region.

TABLE I. Experimental spectroscopic constants of fenchone.

Parameter	
A^a (MHz)	1555.750 82(27)^b
B (MHz)	1168.264 37(25)
C (MHz)	961.419 07(25)
Δ_J (kHz)	0.0343(69)
Δ_{JK} (kHz)	−0.0312
Δ_K (kHz)	0.0387(32)
δ_J (kHz)	0.00467(36)
δ_K (kHz)	0.0448(30)
$a/b/c^c$ (D)	y/y/y
σ^d (kHz)	4.7
N^e	150

^{a}A, B, and C are the rotational constants; Δ_J, Δ_{JK}, Δ_K, δ_J, and δ_K are the centrifugal distortion constants.
^{b}Standard error in parentheses in units of the last digit.
^{c}Yes (y) or no (n) observation of a-, b-, and c-type transitions.
$^d\sigma$ is the rms deviation of the fit.
^{e}N is the number of the fitted transitions.

TABLE II. Calculated spectroscopic parameters of fenchone.

Parameter	6-311++G(d,p)					
	MP2		B3LYP		M062X	
A^a (MHz)	1558.5	0.2%[b]	1551.2	−0.5%	1563.4	0.8%
B (MHz)	1172.2	0.3%	1157.0	−1.0%	1175.9	0.8%
C (MHz)	964.5	0.3%	955.1	−0.6%	966.7	0.5%
$\mu_a/\mu_b/\mu_c{}^c$ (D)	0.1/2.5/1.2		0.2/2.8/1.2		0.1/2.8/1.1	

Parameter	Cc-pVTZ					
	MP2		B3LYP		M062X	
A^a (MHz)	1568.1	0.8%[b]	1558.2	0.2%	1569.3	0.9%
B (MHz)	1182.4	0.9%	1162.3	−0.5%	1181.1	1.1%
C (MHz)	971.5	0.7%	959.4	−0.2%	970.9	1.0%
$\mu_a/\mu_b/\mu_c{}^c$ (D)	0.1/2.5/1.0		0.1/2.6/1.1		0.1/2.7/1.1	

Parameter	Aug-cc-pVTZ					
	MP2		B3LYP		M062X	
A^a (MHz)	1566.8	0.7%[b]	1558.3	0.2%	1570.0	0.9%
B (MHz)	1181.7	1.1%	1162.0	−0.5%	1180.6	1.1%
C (MHz)	971.2	1.0%	959.1	−0.2%	970.7	1.0%
$\mu_a/\mu_b/\mu_c{}^c$ (D)	0.1/2.7/1.1		0.1/2.8/1.2		0.1/2.8/1.1	

[a] A, B, and C are the rotational constants.

[b] Deviation from the experiment; calculated as $(A_{calc} - A_{exp})/A_{exp} \times 100\%$.

[c] μ_a, μ_b, and μ_c are the electric dipole moment components along the principal inertial axes.

dihedral angles for the rotation of the methyl groups at the MP2/6-311++(d,p) level of theory (see Fig. S1 in the supplementary material). The barrier heights obtained were of 900 cm^{-1} (10.8 kJ mol^{-1}), 1000 cm^{-1} (12.0 kJ mol^{-1}), and 1150 cm^{-1} (13.8 kJ mol^{-1}), for the C_8, C_9, and C_{10} methyl groups, respectively. The methyl group internal rotational splittings predicted with these barriers, using the program XIAM,[28] are smaller than 1 kHz and therefore not resolvable in our experiment. Related molecules such as camphor,[16] α- and β-pinene,[29] and nopinone,[29] with similar predicted

methyl internal rotation barriers, do not show internal rotation splittings in their spectra.

B. Structural determination

The determined rotational constants for the parent and all ^{13}C and ^{18}O isotopic species of fenchone allowed the calculation of the coordinates of all heavy atoms using Kraitchman's equations[30] and the program KRA.[31] Two of the carbon atoms are positioned close to one of the principal axes, returning imaginary values of the coordinates after applying Kraitchman's equations. Specifically, these were the a coordinate of C_2 and the b coordinate of C_3. In these cases the values of the coordinates have been set to zero to determine structural parameters. The coordinates (see Table S13 in the supplementary material), all of them carrying Costain's error[32] to give a better account of vibration-rotation effects, were used to obtain the substitution (r_s) structure of Table IV. Since Kraitchman's equations only provide the absolute value of the coordinates, the signs were taken from *ab initio* calculations. The signs of atomic coordinates were consistent across all theoretical methods and basis sets used, except for the b coordinate of C_3, which is calculated to range between −0.0023 and +0.0035 and was set to zero to determine the substitution structure.

Given the limitations of the Kraitchman analysis, the effective structure r_0 of fenchone has also been determined through least-squares fit of the experimental moments of inertia of the observed isotopologues using the program STRFIT.[31] With the rotational constants of all isotopologues of the heavy atom framework, it is possible to determine the
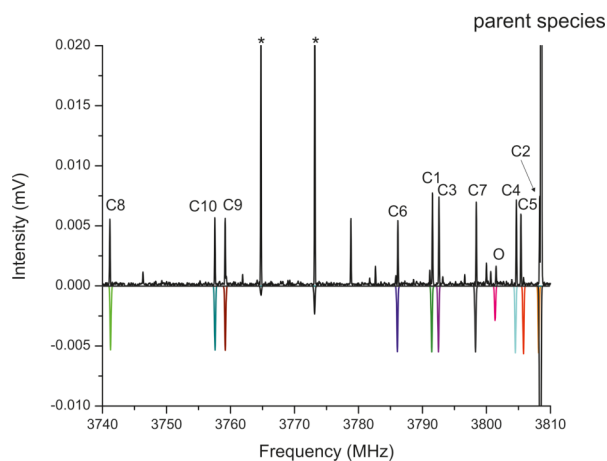

FIG. 5. Rotational spectrum of fenchone from 3740 to 3810 MHz. The figure shows the lines corresponding to the $2_{0,2} \leftarrow 1_{1,1}$ transition of the parent species and ^{13}C and ^{18}O isotopologues in natural abundance. The asterisks indicate other transitions of the parent species.

TABLE III. Experimental spectroscopic constants for the ^{13}C and ^{18}O isotopologues of fenchone.

	$^{13}C_1$	$^{13}C_2$	$^{13}C_3$	$^{13}C_4$	$^{13}C_5$	$^{13}C_6$
A^{a} (MHz)	1555.615 50(41)[b]	1551.525 15(29)	1555.760 85(26)	1546.446 69(37)	1535.945 82(24)	1547.237 00(32)
B (MHz)	1164.060 11(37)	1168.169 27(25)	1164.324 14(22)	1166.654 57(31)	1167.386 03(22)	1160.970 96(25)
C (MHz)	958.560 72(41)	959.948 99(25)	958.768 37(25)	958.159 37(31)	954.196 02(22)	956.378 57(28)
σ^{c} (kHz)	6.5	4.6	4.6	5.9	4.2	5.4
N^{d}	27	29	33	30	31	32

	$^{13}C_7$	$^{13}C_8$	$^{13}C_9$	$^{13}C_{10}$	^{18}O
A (MHz)	1545.305 80(25)	1550.580 04(25)	1546.965 84(30)	1549.680 69(28)	1513.310 97(77)
B (MHz)	1161.923 77(19)	1151.650 01(21)	1153.118 48(25)	1153.100 27(24)	1165.593 49(50)
C (MHz)	959.663 12(21)	948.432 31(22)	952.931 66(25)	953.266 70(24)	946.747 44(57)
σ (kHz)	4.1	4.1	4.8	4.5	5.7
N	31	30	30	30	14

[a]A, B, and C are the rotational constants. The centrifugal distortion constants were fixed to the values obtained for the parent species.
[b]Standard error in parentheses in units of the last digit.
[c]σ is the rms deviation of the fit.
[d]N is the number of fitted transitions.

internal coordinates of these atoms, 27 parameters in total (10 bond lengths, 9 angles, and 8 dihedral angles), also shown in Table IV. The non-floated parameters of the hydrogen atoms were fixed at the values predicted by MP2/6-311++G(d,p) theory. The fit has a standard deviation of 0.0092 uÅ^2 and returns relatively large uncertainties for the distances of r(C$_2$—C$_3$) and r(C$_3$—C$_4$), and the ∠OC$_2$C$_3$ and ∠C$_{10}$C$_3$C$_4$ (see Table IV). Adopting a planar structure around the carbonyl group, a strategy followed for the related terpenoid camphor,[16] did not help improve the quality of the fit. Reducing the number of floating parameters decreases the standard deviation of the fit, at the expense of including more theoretically predicted internal coordinates, but the values of the floated parameters remain essentially the same. Several fits to determine the mass-dependent structure r_m, which is usually close to the equilibrium structure, were also attempted. However, none of the parameters that account for the isotope-dependent rovibrational contributions to the moments of inertia[33] could be determined.

The experimental r_s and r_0 structural parameters are in good agreement, and they correspond well with the r_e equilibrium bond lengths and angles (see Table IV). A comparison between the substitution structure and the *ab initio* MP2 structure, showing the fine match of the experimental and predicted atomic coordinates, is shown in Fig. 6. Several r_0 and MP2 bond lengths and angles, discussed below, are also indicated in Fig. 6. There are a few discrepancies between the r_s and r_0 structures, mainly in the values of the bond lengths involving C$_3$ and the carbons of the methyl groups attached to it. Specifically, the substitution distance r(C$_9$—C$_3$) is quite long while r(C$_{10}$—C$_3$) is very short. There are also some differences between the r_s and r_0 values of the bond lengths in which atom C$_1$ is involved. In both cases, the r_0 values are closer to the theoretically predicted ones, and they are also closer to the experimental bond lengths determined for camphor.[16] The proximity of C$_1$ and C$_3$ to two principal inertial axes (their b and c coordinates are quite small (see Table S13), and the b coordinate of C$_3$ had to be fixed to zero to determine the r_s structure) is likely to be the cause of these differences,

and therefore the r_s structural parameters for these two atoms should be taken with reservation. The r_s and r_0 bond lengths for the C=O are basically identical, and they are extremely close to the theoretical r_e(C=O) bond lengths. Finally, a relatively short r_0(C$_8$—C$_1$) is obtained, which is predicted theoretically with similar values at all levels of theory.

IV. DISCUSSION

The structure of fenchone had been previously studied using X-ray crystallography,[23] and the parameters obtained are displayed alongside the r_s, r_0, and r_e structures determined in this work in Table IV. The values of the X-ray structure differ from the gas phase ones mainly on the distances r(C$_3$—C$_4$) and r(C$_5$—C$_6$), and the dihedral angles τ(C$_3$C$_4$C$_5$C$_6$), τ(C$_4$C$_5$C$_6$C$_1$) and τ(C$_8$C$_1$C$_6$C$_5$). It should be noted that on average the bond distances in the crystal are about 0.007 Å shorter than the r_0 structure. This may be due to the effect of packing forces in the crystal.

The structure of fenchone shows many features common to other bicyclo[2.2.1]heptane derivatives, whose figures and structural parameters are collected in Table IV. In the following discussion we will consider the r_0 structures of all derivatives as the r_s structures present some limitations. The r_0 parameters obtained for fenchone are in excellent agreement with those determined for the related monoterpenoids camphor[16] and camphene.[17] Most bond distances and angles have effectively the same values, considering their uncertainties. Specifically, the C=O bond lengths in camphor and fenchone show an extremely good match, and the same occurs with the unusually short distance C$_8$—C$_1$ involving the methyl substituent at C$_1$. The changes in the methyl group positions in going from camphor to fenchone do not seem to affect the carbon-carbon distances within the bicyclic ring, confirming its rigidity. The only exceptions are the angles ∠C$_3$C$_4$C$_5$, which is more acute (by ca. 4°) in camphor than in fenchone and camphene, and ∠C$_7$C$_1$C$_6$, which is more obtuse by ca. 2° in camphor than in fenchone and camphene. This is

TABLE IV. Comparison of the bond lengths (in Å) and angles (in degrees) of the heavy atoms of fenchone determined experimentally and theoretically, and with those of related molecules.

	Fenchone				Camphor[a]	Camphene[b]	Norbornane[c]
	r_s	r_0[d]	X-ray[e]	MP2			
$r(C_1-C_6)$	1.521(13)	1.555(18)	1.550(6)	1.559	1.557(6)	1.556(5)	1.536(15)
$r(C_1-C_2)$	1.512(11)	1.526(29)[f]	1.517(5)	1.522	1.537(10)	1.510(8)	1.536(15)
$r(C_2-C_3)$	1.545(14)	1.535(31)	1.526(5)	1.538	1.530(3)	1.527(5)	1.573(15)
$r(C_3-C_4)$	1.565(17)	1.549(30)	1.517(5)	1.550	1.545(5)	1.555(7)	1.536(15)
$r(C_4-C_5)$	1.531(4)	1.546(8)	1.537(5)	1.541	1.547(4)	1.546(6)	1.536(15)
$r(C_5-C_6)$	1.566(5)	1.562(9)	1.542(6)	1.557	1.564(6)	1.562(5)	1.573(15)
$r(C_7-C_1)$	1.536(13)	1.541(25)	1.547(6)	1.541	1.543(8)	1.544(6)	1.546(24)
$r(C_7-C_4)$	1.541(3)	1.552(8)[f]	1.547(6)	1.544	1.555(8)	1.550(7)	1.546(24)
$r(C_8-C_1)$	1.537(7)	1.521(11)	1.518(6)	1.513	1.522(4)	...	...
$r(C_9-C_3)$	1.568(18)	1.545(16)	1.538(6)	1.537	...	1.541(10)	...
$r(C_{10}-C_3)$	1.504(18)	1.535(13)	1.524(5)	1.531	...	1.543(12)	...
$r(O-C_2)$	1.213(3)	1.214(5)	1.215(4)	1.218	1.212(2)	...	...
$r(C_2=C)$	...	...	...	...	...	1.340(6)	...
$\angle(C_1C_6C_5)$	103.6(3)	103.9(7)	104.5(3)	104.30	103.8(3)	103.1(3)	102.71
$\angle(C_1C_2C_3)$	107.2(7)	107.5(12)[f]	107.6(3)	107.5	105.8(2)	106.9(5)	102.71
$\angle(C_2C_3C_4)$	99.7(4)	100.8(9)	101.0(3)	100.70	101.6(1)	101.1(4)	102.71
$\angle(C_3C_4C_5)$	109.3(8)	110.3(8)	110.4(3)	110.37	106.5(3)	110.8(6)	108.97
$\angle(C_4C_5C_6)$	102.46(15)	102.8(3)	102.9(3)	102.69	102.6(1)	103.1(3)	102.71
$\angle(C_7C_1C_6)$	103.0(7)	101.4(11)	101.2(3)	100.76	103.0(6)	101.1(3)	102.04(6)
$\angle(OC_2C_3)$	124.5(13)	125.8(31)	125.8(3)	125.53	126.8(1)	126.7(3)	...
$\angle(C_8C_1C_6)$	115.9(5)	115.3(11)	115.4(3)	115.29	114.8(3)	...	...
$\angle(C_9C_3C_4)$	109.6(13)	111.4(14)	110.8(3)	111.43	...	110.2(9)	...
$\angle(C_{10}C_3C_4)$	117.4(13)	116.2(22)	115.9(3)	115.91	...	113.9(6)	...
$\angle(C_1C_7C_4)$	94.4(3)	95.2(6)[f]	95.2(3)	95.6	94.5(4)	94.2(2)	93.41(9)
$\tau(C_2C_3C_4C_5)$	72.3(11)	70.2(13)	70.4(4)	70.2	...	...	...
$\tau(C_3C_4C_5C_6)$	−68.1(5)	−67.3(10)	−65.3(4)	−67.2	...	...	...
$\tau(C_4C_5C_6C_1)$	−5.7(5)	−5.9(9)	−7.8(4)	−6.1	...	...	...
$\tau(C_7C_1C_6C_5)$	−30.3(4)	−30.3(7)	−28.5(4)	−29.9	...	...	...
$\tau(C_8C_1C_6C_5)$	−161.0(7)	−160.6(16)	−158.0(3)	−161.4	...	...	...
$\tau(C_9C_3C_4C_7)$	79.8(6)	80.4(11)	81.4(4)	80.6	...	...	...
$\tau(C_{10}C_3C_4C_2)$	−122.2(18)	−119.7(15)	...	−119.0	...	...	...
$\tau(OC_2C_3C_4)$	−178.3(6)	−177.7(10)	−178.9(4)	−177.5	...	...	...

[a]Reference 16.
[b]Reference 17.
[c]Reference 34.
[d]Non-fitted parameters were fixed to the MP2/6-311++G(d,p) values.
[e]Reference 23.
[f]These parameters were not fitted directly using STRFIT but derived from the obtained r_0 structure.

likely to be related to the absence of methyl groups at C_3 and their presence at C_7 in camphor.

Fenchone, camphor and camphene are all norbornane derivatives, and their structural parameters can be examined with relation to those of norbornane[34] (see Table IV). Norbornane is an archetypical molecule for strained bond lengths and angles. The bicyclic skeleton of norbornane forces the six-membered ring into a boat configuration and results in angles considerably smaller than those usually found for singly bonded (sp³) carbon atoms, and C—C bonds longer or shorter than the typical C—C bond length. In particular, the angle involving the bridge carbon C_7 is quite strained, with a value of 93.41(9)°. Due to its C_{2v} symmetry, norbornane

has three different C—C bond lengths (see Table IV). In going from norbornane to camphene, camphor and fenchone, the most important change is the addition of an unsaturated substituent (=CH₂) or a carbonyl group (=O) at C_2, thereby modifying the character of the C_2 carbon and giving rise to significant structural adjustments. The most drastic effect occurs on the C_2—C_3 bond length, which is reduced by ca. 3% from 1.573(15) Å in norbornane to values around 1.530 Å in the three norbornane derivatives. Other bond lengths in the six-membered rings of fenchone, camphor, and camphene are also modified: the C_5—C_6 bond length also decreases, but to a much lesser extent (ca. 0.7%); the C_1—C_6, C_3—C_4, and C_4—C_5 bonds are elongated by about 1%, with very
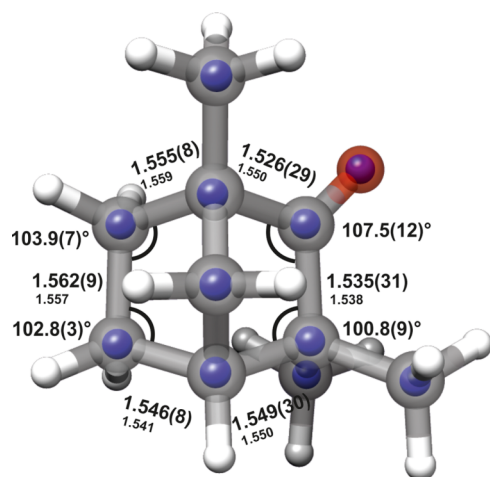
FIG. 6. Comparison of the *ab initio* MP2 structure of fenchone (full molecular drawing) with the r_s atom coordinates (the blue spheres represent the C atoms and the purple sphere represents the O atom, all from Kraitchman analysis). The r_0 (top) and MP2 (bottom) values of selected bond lengths (in Å) and angles of fenchone are also indicated on the figure.

similar values for the three substituted [2.2.1] bicyclic monoterpenoids; the C_1—C_2 bond is shortened by about 2% in camphene, while it is basically unchanged for fenchone and camphor, a reflection of the different C_2 substituent. In contrast, the bond lengths involving the bridge carbon C_7 do not suffer large variations. The value of $r(C_1—C_7)$ and $r(C_4—C_7)$ is effectively the same for the three substituted norbornanes, with a slight increase for $r(C_4—C_7)$ with respect to norbornane, which breaks the symmetry in the bridge carbon parameters.

There is a remarkable consistency in the bond lengths values of the three substituted norbornanes fenchone, camphor, and camphene. The changes with respect to norbornane bond lengths follow the same trend and they focus on the six-membered ring because of the need of minimising ring strain after the introduction of an unsaturated substituent at C_2. The bond angles of the three substituted monoterpenoids also experience some variations with respect to norbornane, and mostly they vary in the same way. The largest change occurs for the $\angle C_1C_2C_3$ angle, which increases by 3°-4° with respect to norbornane. Angle $\angle C_2C_3C_4$ decreases by ca. 1%, while angles $\angle C_1C_6C_5$ and $\angle C_4C_5C_6$ are essentially the same considering their uncertainties. For the bond angles $\angle C_3C_4C_5$ and $\angle C_7C_1C_6$ the behavior of the camphor differs with respect to fenchone and camphene, which may be related to the different position of the methyl substituents, as indicated previously. Angle $\angle C_3C_4C_5$ increases by ca. 1% for fenchone and camphene with respect to norbornane, while it decreases by ca. 2% for camphor. The opposite behavior is observed for angle $\angle C_7C_1C_6$. The angle involving the bridge carbon $\angle C_1C_7C_4$ increases by ca. 1%-2% in the three norbornane derivatives but continues to be strained, with the largest value being 95.2(6)° for fenchone.

The structural adjustments in fenchone result in a twist in its six-membered ring such that the bonds C_2—C_3 and C_5—C_6 are not parallel like in norbornane (see Fig. 6). This twist has

been observed for camphor,[16] and has also been reported for other substituted norbornanes and camphanes, where it was tentatively related to the presence of a substituent in C_2.[35]

V. CONCLUSIONS

The broadband rotational spectrum of fenchone has been observed for the first time and the rotational constants of the parent, all ^{13}C and ^{18}O species have been determined. Theoretical predictions with several density functional and *ab initio* methods and with different basis sets have been performed. All methods provide satisfactory values of the rotational constants. The best agreement between theory and experiment was provided by the MP2/6-311++G(d,p) level of theory, with differences of 0.3% or lower for the three rotational constants, followed by B3LYP with the cc-pVTZ and aug-cc-pVTZ basis sets, which perform similarly with differences between equilibrium and ground-state rotational constants lower than 0.5%.

The substitution and r_0 structures of fenchone have been determined, and the latter has been compared with those previously reported for norbornane and the norbornane derivatives camphor and camphene, both with substituents at C_2 like fenchone. The structure of fenchone is remarkably similar to those of camphor and camphene. Comparison with camphor allows identification of changes in $\angle CCC$ angles due to the different position of the methyl groups. All norbornane derivatives display similar structural changes with respect to norbornane. These changes mainly affect the bond lengths and angles of the six-membered rings, indicating that the substituent at C_2 drives structural adjustments to minimise ring strain after its introduction.

Rotational spectroscopy has demonstrated to be a powerful technique to determine molecular structure. The development of broadband rotational spectroscopy and the improved accessibility to lower frequency regions of the rotational spectrum makes it possible to tackle larger molecules.[20,36,37] In this context, the determination of the structure of fenchone will pave the way to study its complexes with water and other molecules, shedding light on the interactions that this molecule establishes in processes involving living organisms and the environment.

SUPPLEMENTARY MATERIAL

See supplementary material for Tables S1-S12, with the observed frequencies and residuals for the rotational transitions of the parent and all observed isotopologues of fenchone; Table S13 with the substitution coordinates of the heavy atoms of fenchone; Figure S1, with the internal rotation barriers for the methyl groups of fenchone calculated at the MP2/6-311++G(d,p) level of theory.

ACKNOWLEDGMENTS

[1]G. Wang, W. Tang, and R. R. Bidigare, in *Natural Products: Drug Discovery and Therapeutic Medicine*, edited by L. Zhang and A. L. Demain (Humana Press Inc., Totowa, NJ, 2005), pp. 197–227.

[2]P. K. Ajikumar, K. Tyo, S. Carlsen, O. Mucha, T. Heng Phon, and G. Stephanopoulos, Mol. Pharm. **5**, 167 (2008).

[3]C. Sell, *The Chemistry of Fragrances*, 2nd ed. (RSC Publishing, 2006).

[4]M. Hallquist *et al.*, Atmos. Chem. Phys. **9**, 5155 (2009).

[5]R. Chizzola, in *Natural Products*, edited by K. G. Ramawat and J. M. Mérillon (Springer-Verlag Berlin, Heidelberg, 2013), pp. 2973–3008.

[6]J. H. Krolla and J. H. Seinfeld, Atmos. Environ. **42**, 3593 (2008).

[7]G. G. Brown, B. C. Dian, K. O. Douglass, S. M. Geyer, S. T. Shipman, and B. H. Pate, Rev. Sci. Instrum. **79**, 053193 (2008).

[8]R. Kotan, S. Kordali, and A. Cakir, Z. Naturforsch. **62c**, 507 (2007).

[9]A. S. Fouda, S. M. Rashwan, and H. A. Abo-Mosallam, Desalin. Water Treat. **52**, 5175 (2014).

[10]A. A. Ceacero-Vega, B. Ballesteros, I. Bejan, I. Barnes, E. Jiménez, and J. Albaladejo, J. Phys. Chem. A **116**, 4097 (2012).

[11]J. R. Avilés Moreno, T. R. Huet, and J. J. López González, Struct. Chem. **24**, 1163 (2013).

[12]D. Schmitz, V. A. Shubert, B. M. Giuliano, and M. Schnell, J. Chem. Phys. **141**, 034304 (2014).

[13]D. Schmitz, V. A. Shubert, T. Betz, and M. Schnell, Front. Chem. **3**, 15 (2015).

[14]H. V. L. Nguyen, H. Mouhib, S. Klahm, W. Stahl, and I. Kleiner, Phys. Chem. Chem. Phys. **15**, 10012 (2013).

[15]J. R. Avilés Moreno, F. Partal Ureña, J. J. López González, and T. R. Huet, Chem. Phys. Lett. **473**, 17 (2009), peryllaldehyde.

[16]Z. Kisiel, O. Desyatnyk, E. Bialkowska-Jaworska, and L. Pszczólkowski, Phys. Chem. Chem. Phys. **5**, 820 (2003).

[17]E. M. Neeman, P. Dréan, and T. R. Huet, J. Mol. Spectrosc. **322**, 50 (2016).

[18]S. Ghosh and S. Banerjee, ARKIVOC **vii**, 8 (2002).

[19]D. Loru, I. Peña, J. L. Alonso, and M. E. Sanz, Chem. Commun. **52**, 3615 (2016).

[20]N. A. Seifert, C. Pérez, J. L. Neill, B. H. Pate, M. Vallejo-López, A. Lesarri, E. J. Cocinero, and F. Castaño, Phys. Chem. Chem. Phys. **17**, 18282 (2015).

[21]V. Vaquero, M. E. Sanz, J. C. López, and J. L. Alonso, J. Phys. Chem. A **111**, 3443 (2007).

[22]C. Pérez, M. T. Muckle, D. P. Zaleski, N. A. Seifert, B. Temelso, G. C. Shields, Z. Kisiel, and B. H. Pate, Science **336**, 897 (2012).

[23]A. D. Bond and J. E. Davies, Acta Crystallogr., Sect. E: Struct. Rep. Online **57**, o1034 (2001).

[24]J. L. Neill, S. T. Shipman, L. Alvarez-Valtierra, A. Lesarri, Z. Kisiel, and B. H. Pate, J. Mol. Spectrosc. **269**, 21 (2011).

[25]S. A. Cooke and P. Ohring, J. Spectrosc. 698392 (2013).

[26]J. K. G. Watson, in *Vibrational Spectra and Structure*, edited by J. R. Durig (Elsevier, New York, 1977), Vol. 6, pp. 1–78.

[27]H. M. Pickett, J. Mol. Spectrosc. **148**, 371 (1991).

[28]H. Hartwig and H. Dreizler, Z. Naturforsch., A: Phys. Sci. **51**, 923 (1996).

[29]J.-R. Aviles-Moreno, E. Neeman, and T. R. Huet, "Microwave spectroscopy of monoterpenes of atmospheric interest: α-pinene, β-pinene, and nopinone," in *International Symposium on Molecular Spectroscopy*, *Talk WJ14, Champaign-Urbana, USA* (2014).

[30]J. Kraitchman, Am. J. Phys. **21**, 17 (1953).

[31]Z. Kisiel, PROSPE—Programs for ROtational SPEctroscopy, http://info.ifpan.edu.pl/~kisiel/prospe.htm; accessed 1 February 2016.

[32]C. C. Costain, Trans. Am. Cryst. Assoc. **2**, 157 (1966).

[33]J. K. G. Watson, A. Roytburg, and W. Ulrich, J. Mol. Spectrosc. **196**, 102 (1999).

[34]L. Doms *et al.*, J. Am. Chem. Soc. **105**, 158 (1983).

[35]C. Altona and M. Sundaralingan, J. Am. Chem. Soc. **92**, 1995 (1970).

[36]N. A. Seifert, A. L. Steber, J. L. Neill, C. Pérez, D. P. Zaleski, B. H. Pate, and A. Lesarri, Phys. Chem. Chem. Phys. **15**, 11468 (2013).

[37]I. Peña, C. Cabezas, and J. L. Alonso, Angew. Chem., Int. Ed. **54**, 2991 (2015).